Short-range correlation physics at low RG resolution

Anthony Tropiano[1], Scott Bogner[2], Dick Furnstahl[1]

[1]Ohio State University, [2]Michigan State University

APS DNP Meeting – Virtual Meeting

October 12, 2021

ajt, S.K. Bogner, and R.J. Furnstahl, arXiv:2105.13936

Phys. Rev. C ***104****, 034311 (2021)*

Motivation

- Recent experiments have been able to isolate processes where short-range correlation (SRC) physics is dominant and well accounted for by SRC phenomenology
- SRC physics at high RG resolution
  - SRC pairs are components in the nuclear wave function with relative momenta above the Fermi momentum

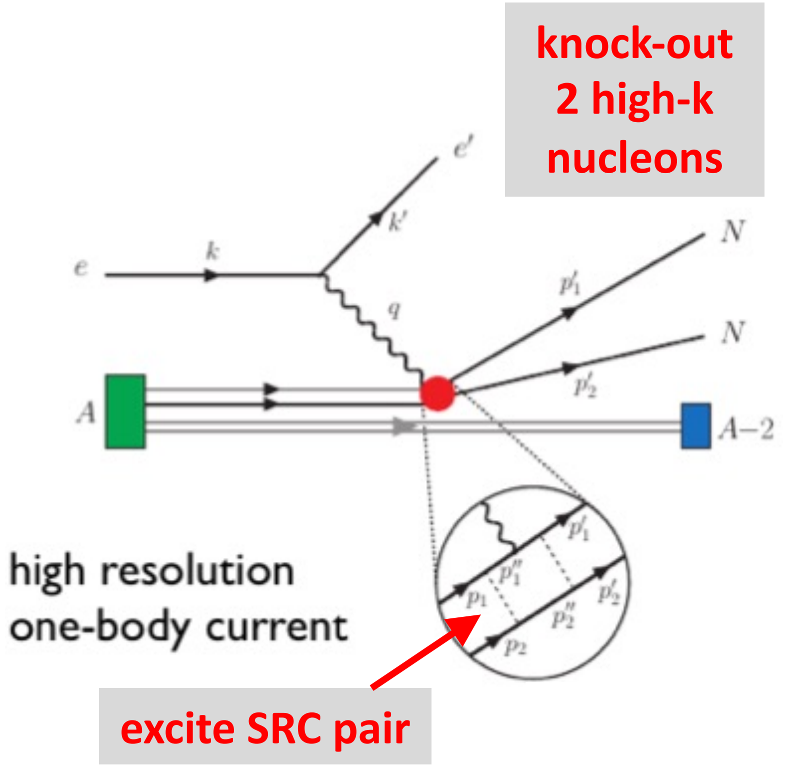

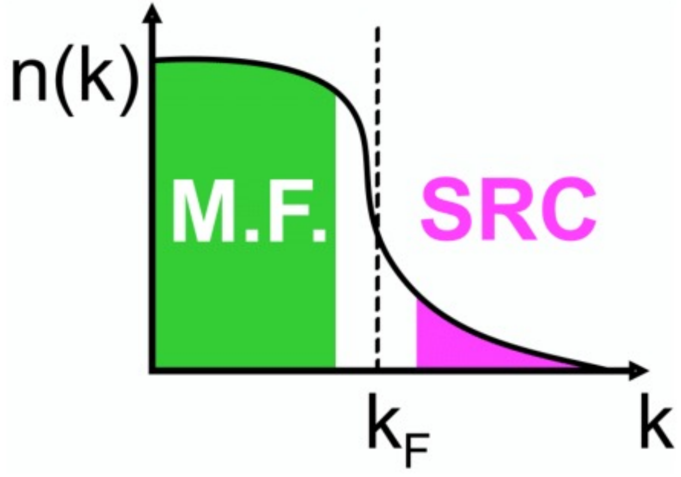

Motivation

- Recent experiments have been able to isolate processes where short-range correlation (SRC) physics is dominant and well accounted for by SRC phenomenology
- SRC physics at low RG resolution
  - The SRC *physics* is shifted into the reaction operators from the nuclear wave function (which becomes soft)
  - Operators do not become hard, which simplifies calculations

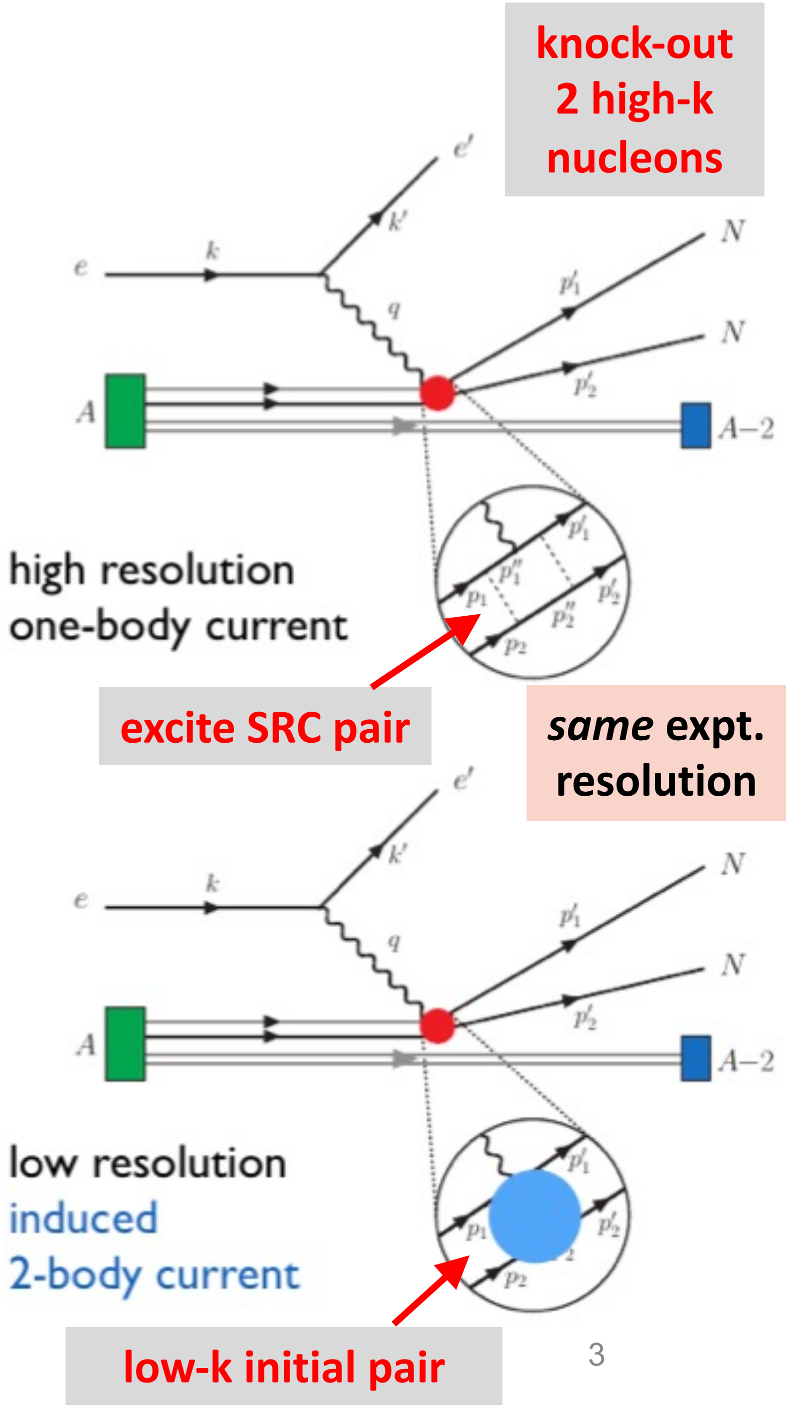

Motivation

- Recent experiments have been able to isolate processes where short-range correlation (SRC) physics is dominant and well accounted for by SRC phenomenology
- SRC physics at low RG resolution
  - The SRC *physics* is shifted into the reaction operators from the nuclear wave function (which becomes soft)
  - Operators do not become hard, which simplifies calculations
- Experimental resolution (set by momentum of probe) is the same in both pictures
- Same observables but different physical interpretation!

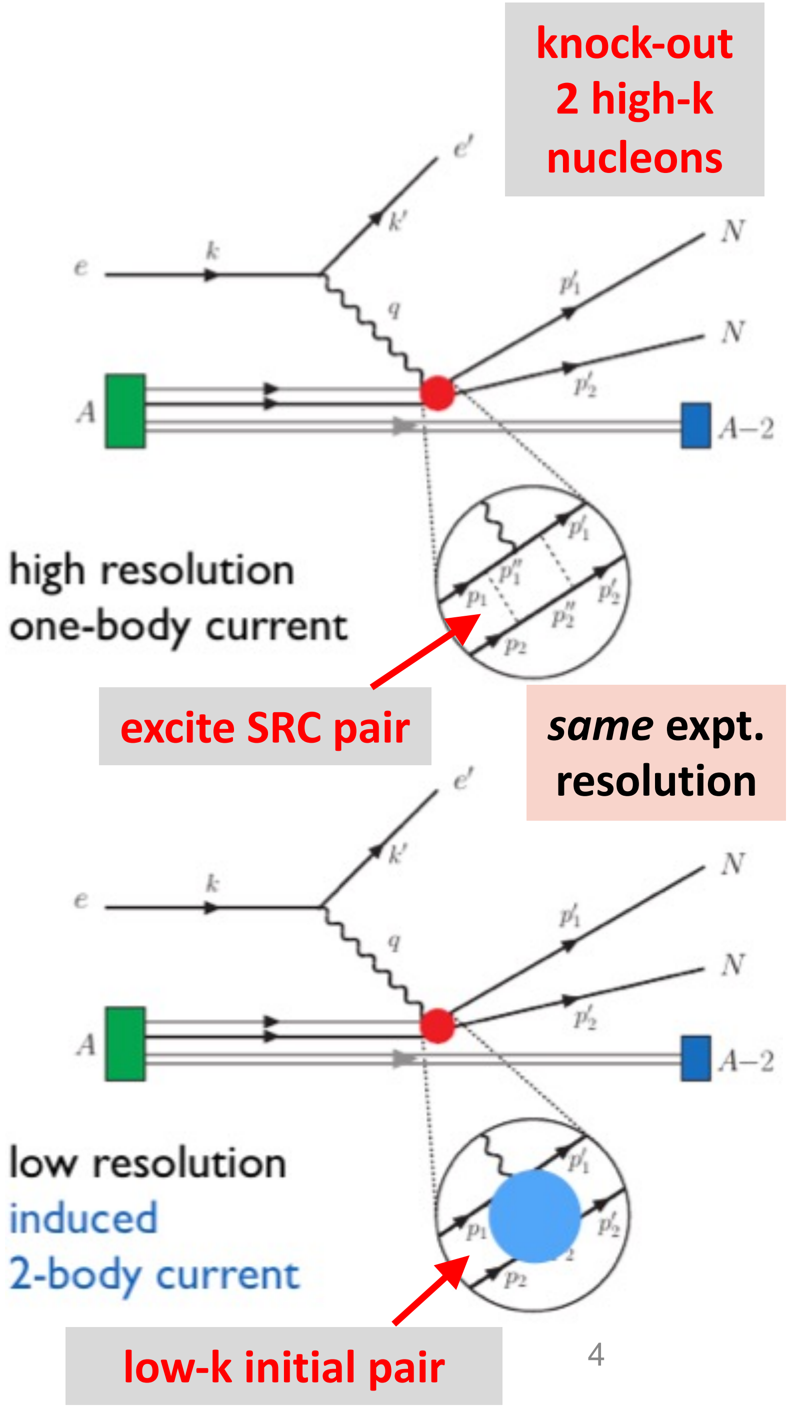

Similarity Renormalization Group (SRG)

- AV18 wave function has significant SRC
- What happens to the wave function at low RG resolution?
- Use SRG to unitarily evolve to low RG resolution where λ gives the decoupling scale

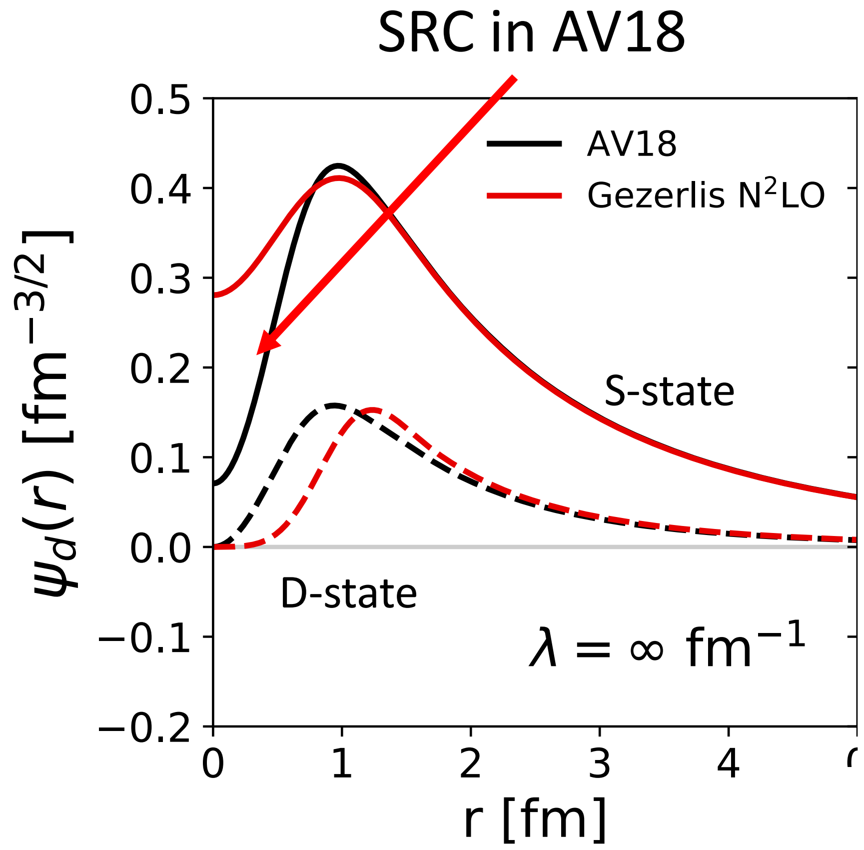

Fig. 1: SRG evolution of deuteron wave function in coordinate space for AV18 and Gezerlis N^{2}LO[1].

[1]A. Gezerlis et al., Phys. Rev. C **90**, 054323 (2014)

Similarity Renormalization Group (SRG)

- SRC physics in AV18 is gone from wave function at low RG resolution
- Deuteron wave functions become soft and D-state probability goes down
- Observables such as asymptotic D-S ratio are the same

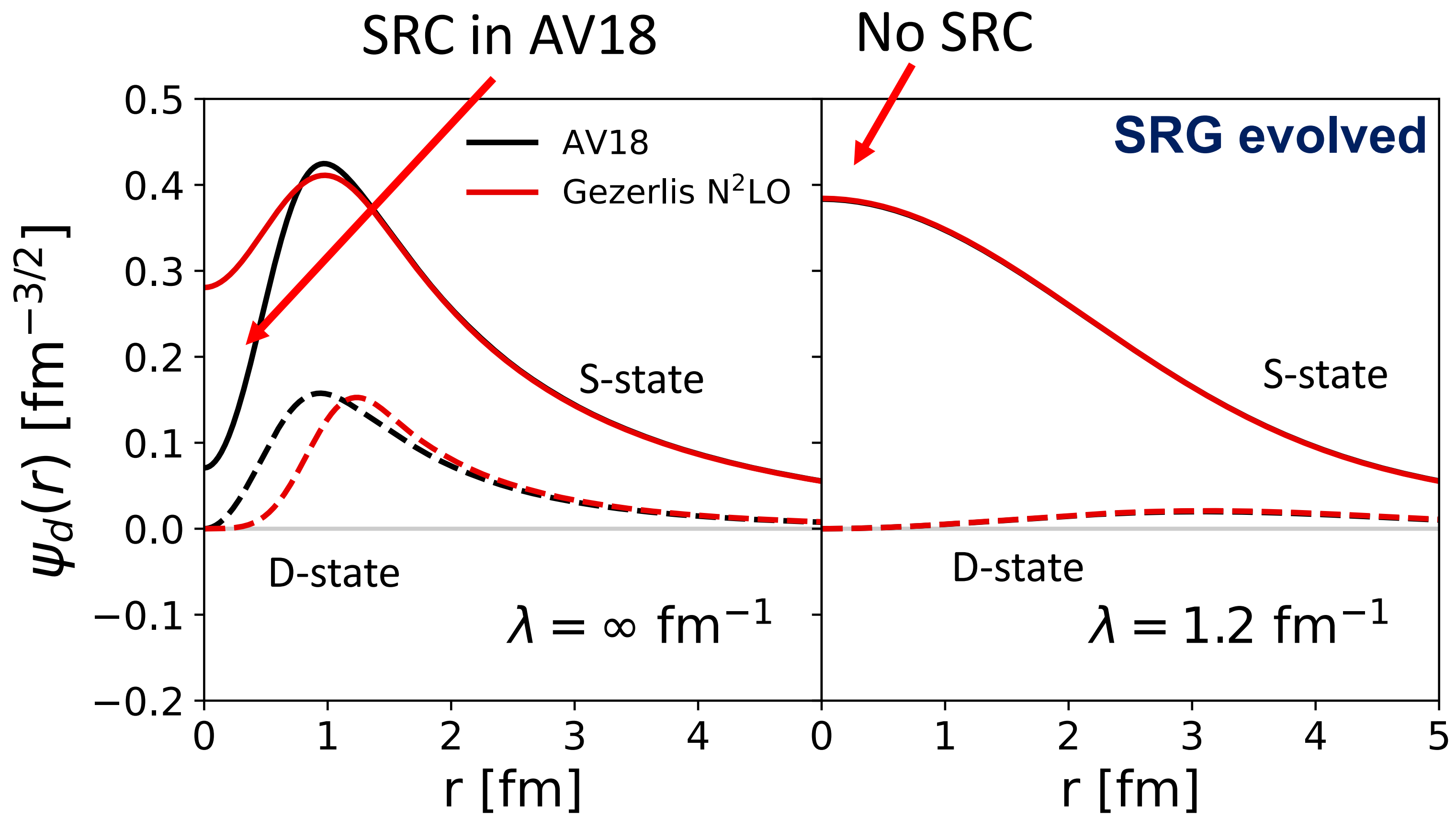

Fig. 1: SRG evolution of deuteron wave function in coordinate space for AV18 and Gezerlis N^{2}LO[1].

[1]A. Gezerlis et al., Phys. Rev. C **90**, 054323 (2014)

Momentum distributions at low RG resolution

- Soft wave functions at low RG resolution
  - Where does the SRC physics go?

Momentum distributions at low RG resolution

- Soft wave functions at low RG resolution
  - Where does the SRC physics go?
- SRC physics shifts to the operators

$$\langle \psi_f^{hi} | U_\lambda^\dagger U_\lambda O^{hi} U_\lambda^\dagger U_\lambda | \psi_i^{hi} \rangle = \langle \psi_f^{low} | O^{low} | \psi_i^{low} \rangle$$

- Apply SRG transformations to momentum distribution operator

$$n^{hi}(\boldsymbol{q}) = a_{\boldsymbol{q}}^\dagger a_{\boldsymbol{q}}$$

$$U_\lambda = 1 + \frac{1}{4} \sum_{\boldsymbol{K},\boldsymbol{k},\boldsymbol{k}'} \delta U_\lambda^{(2)}(\boldsymbol{k}, \boldsymbol{k}') a_{\frac{\boldsymbol{K}}{2}+\boldsymbol{k}}^\dagger a_{\frac{\boldsymbol{K}}{2}-\boldsymbol{k}}^\dagger a_{\frac{\boldsymbol{K}}{2}-\boldsymbol{k}'} a_{\frac{\boldsymbol{K}}{2}+\boldsymbol{k}'} + \cdots$$

Momentum distributions at low RG resolution

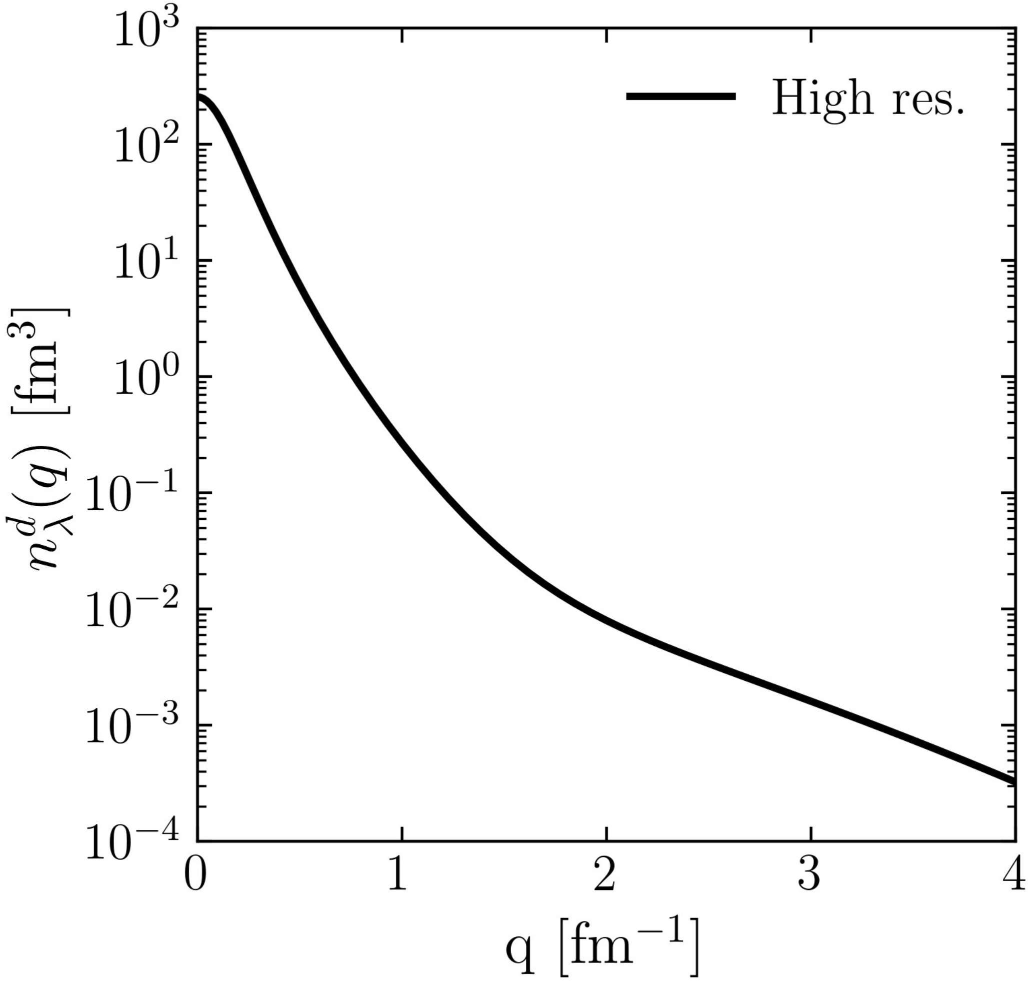

Fig. 2: Contributions to deuteron momentum distribution with AV18 and $\lambda = 1.35$ fm^{-1}.

- Deuteron example

$$n^{lo}(\boldsymbol{q}) = (1 + \delta U) a^\dagger_{\boldsymbol{q}} a_{\boldsymbol{q}} (1 + \delta U^\dagger)$$

$$\langle \psi^{hi}_d | a^\dagger_{\boldsymbol{q}} a_{\boldsymbol{q}} | \psi^{hi}_d \rangle$$

Momentum distributions at low RG resolution

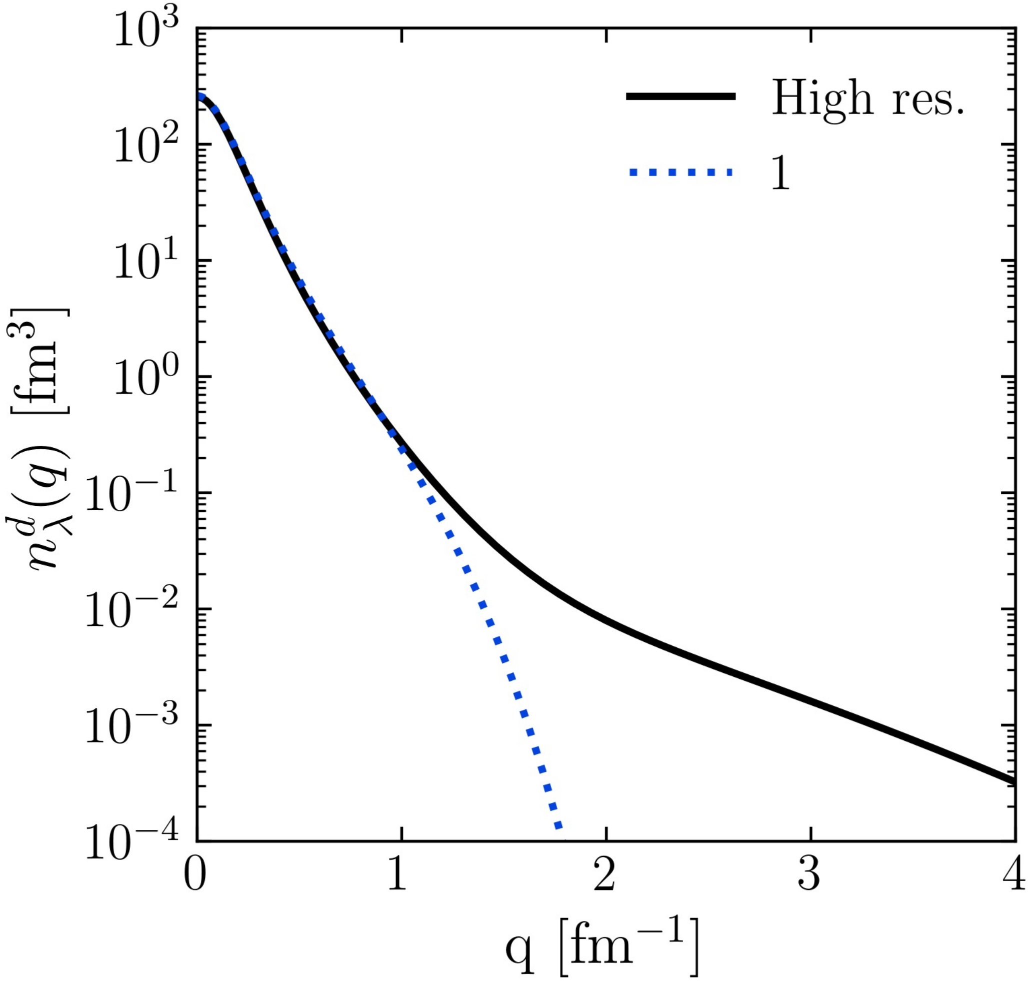

Fig. 2: Contributions to deuteron momentum distribution with AV18 and $\lambda = 1.35$ fm^{-1}.

- Deuteron example

$$n^{lo}(\boldsymbol{q}) = (1 + \delta U) a^\dagger_{\boldsymbol{q}} a_{\boldsymbol{q}} (1 + \delta U^\dagger)$$

$$\langle \psi^{hi}_d | a^\dagger_{\boldsymbol{q}} a_{\boldsymbol{q}} | \psi^{hi}_d \rangle$$

$$\langle \psi^{lo}_d | a^\dagger_{\boldsymbol{q}} a_{\boldsymbol{q}} | \psi^{lo}_d \rangle$$

Momentum distributions at low RG resolution

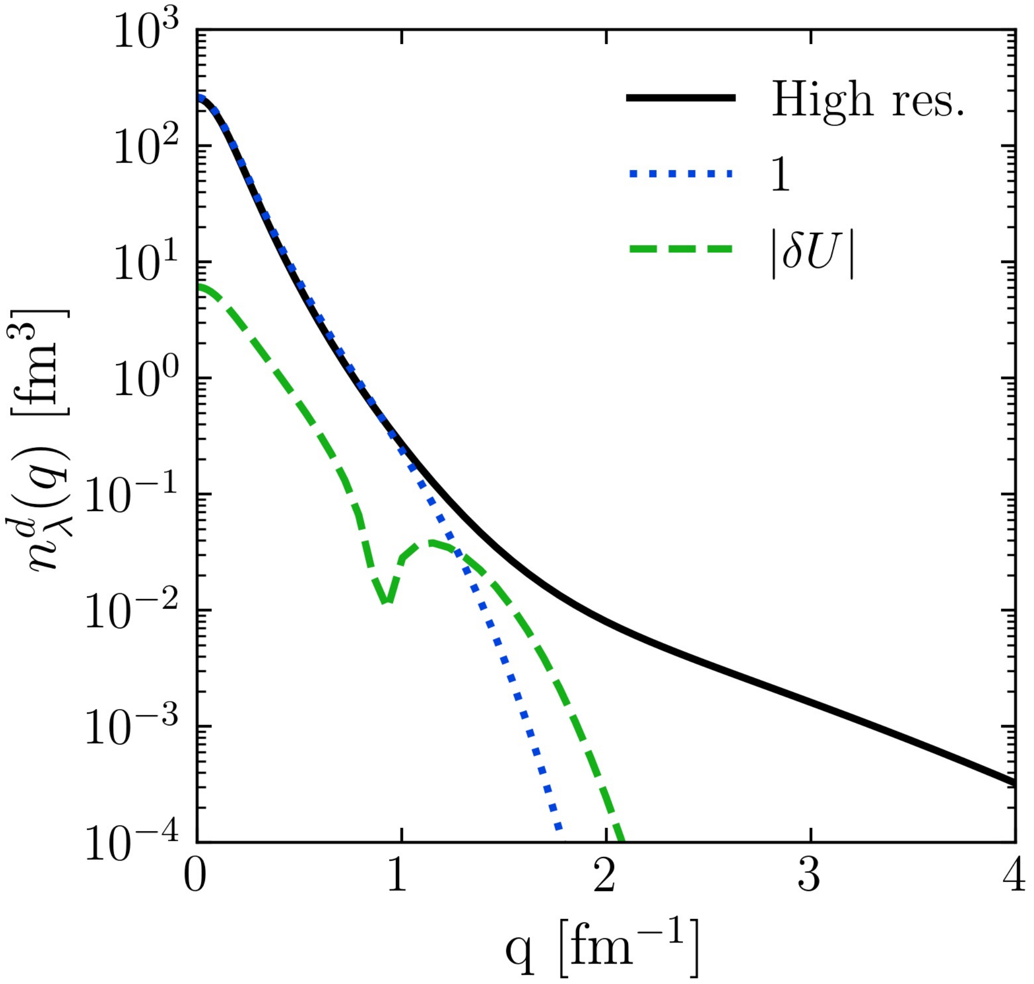

Fig. 2: Contributions to deuteron momentum distribution with AV18 and $\lambda = 1.35$ fm^{-1}.

- Deuteron example

$$n^{lo}(\boldsymbol{q}) = (1 + \delta U) a_{\boldsymbol{q}}^\dagger a_{\boldsymbol{q}} (1 + \delta U^\dagger)$$

$$\langle \psi_d^{hi} | a_{\boldsymbol{q}}^\dagger a_{\boldsymbol{q}} | \psi_d^{hi} \rangle$$

$$\langle \psi_d^{lo} | a_{\boldsymbol{q}}^\dagger a_{\boldsymbol{q}} | \psi_d^{lo} \rangle$$

$$\langle \psi_d^{lo} | \delta U a_{\boldsymbol{q}}^\dagger a_{\boldsymbol{q}} + a_{\boldsymbol{q}}^\dagger a_{\boldsymbol{q}} \delta U^\dagger | \psi_d^{lo} \rangle$$

Momentum distributions at low RG resolution

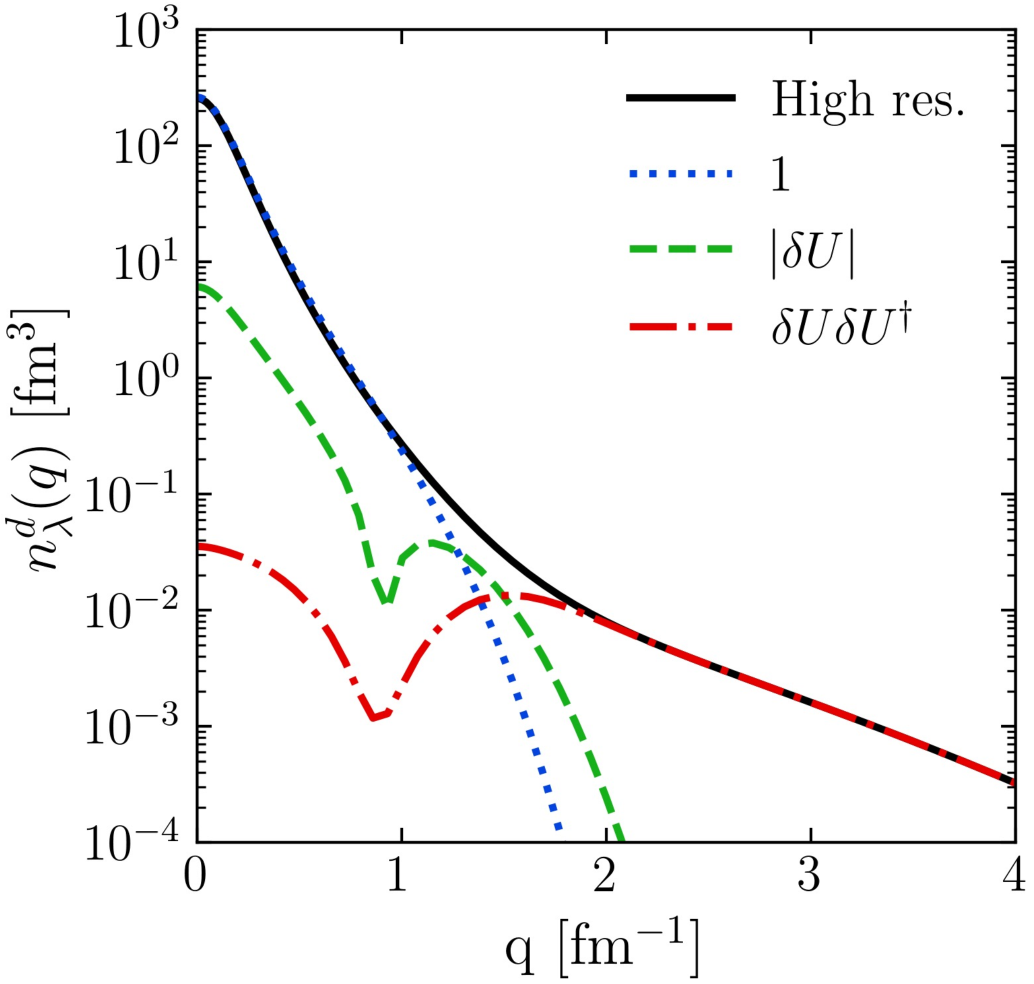

Fig. 2: Contributions to deuteron momentum distribution with AV18 and $\lambda = 1.35$ fm^{-1}.

- Deuteron example

$$n^{lo}(\boldsymbol{q}) = (1 + \delta U) a^\dagger_{\boldsymbol{q}} a_{\boldsymbol{q}} (1 + \delta U^\dagger)$$

$$\langle \psi_d^{hi} | a^\dagger_{\boldsymbol{q}} a_{\boldsymbol{q}} | \psi_d^{hi} \rangle$$

$$\langle \psi_d^{lo} | a^\dagger_{\boldsymbol{q}} a_{\boldsymbol{q}} | \psi_d^{lo} \rangle$$

$$\langle \psi_d^{lo} | \delta U a^\dagger_{\boldsymbol{q}} a_{\boldsymbol{q}} + a^\dagger_{\boldsymbol{q}} a_{\boldsymbol{q}} \delta U^\dagger | \psi_d^{lo} \rangle$$

$$\langle \psi_d^{lo} | \delta U a^\dagger_{\boldsymbol{q}} a_{\boldsymbol{q}} \delta U^\dagger | \psi_d^{lo} \rangle$$

Momentum distributions at low RG resolution

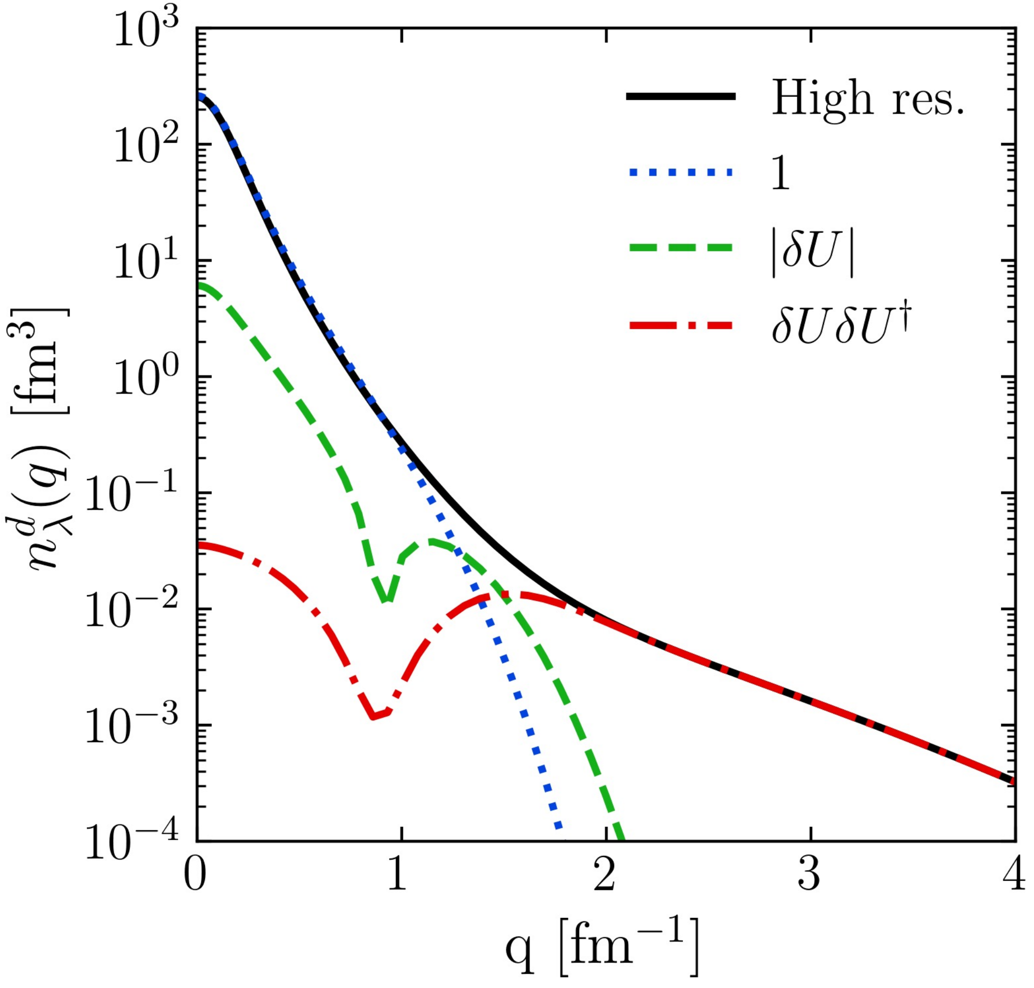

Fig. 2: Contributions to deuteron momentum distribution with AV18 and $\lambda = 1.35$ fm^{-1}.

- For high-q, the $\delta U_\lambda \delta U_\lambda^\dagger$ 2-body term dominates

$$\approx \sum_{\boldsymbol{K},\boldsymbol{k},\boldsymbol{k}'} \delta U_\lambda(\boldsymbol{k},\boldsymbol{q}) \delta U_\lambda^\dagger(\boldsymbol{q},\boldsymbol{k}') a^\dagger_{\frac{\boldsymbol{K}}{2}+\boldsymbol{k}} a^\dagger_{\frac{\boldsymbol{K}}{2}-\boldsymbol{k}} a_{\frac{\boldsymbol{K}}{2}-\boldsymbol{k}'} a_{\frac{\boldsymbol{K}}{2}+\boldsymbol{k}'}$$

Momentum distributions at low RG resolution

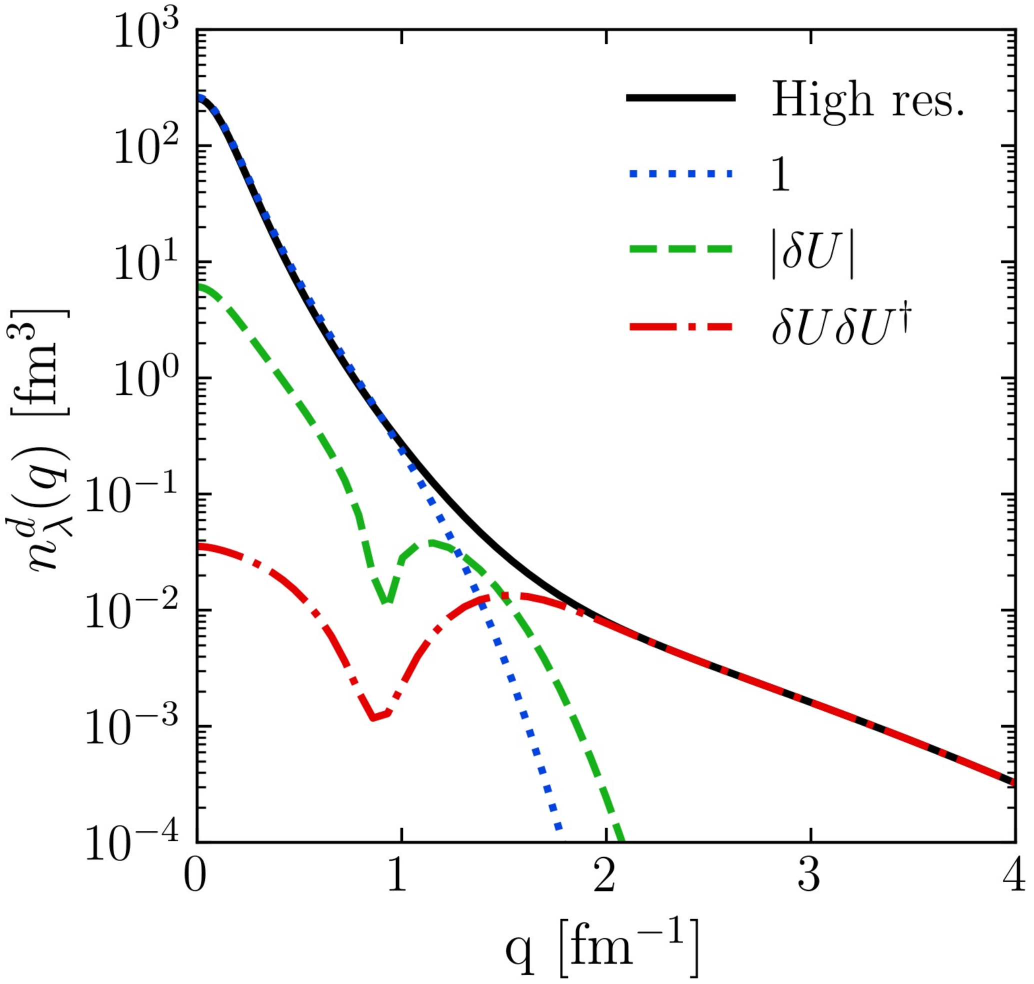

Fig. 2: Contributions to deuteron momentum distribution with AV18 and $\lambda = 1.35$ fm^{-1}.

- For high-q, the $\delta U_\lambda \delta U_\lambda^\dagger$ 2-body term dominates

$$\approx \sum_{\boldsymbol{K},\boldsymbol{k},\boldsymbol{k'}} \delta U_\lambda(\boldsymbol{k},\boldsymbol{q}) \delta U_\lambda^\dagger(\boldsymbol{q},\boldsymbol{k'}) a^\dagger_{\frac{\boldsymbol{K}}{2}+\boldsymbol{k}} a^\dagger_{\frac{\boldsymbol{K}}{2}-\boldsymbol{k}} a_{\frac{\boldsymbol{K}}{2}-\boldsymbol{k'}} a_{\frac{\boldsymbol{K}}{2}+\boldsymbol{k'}}$$

$$\downarrow$$

Factorization: $\delta U_\lambda(\boldsymbol{k},\boldsymbol{q}) \approx F^{lo}_\lambda(\boldsymbol{k}) F^{hi}_\lambda(\boldsymbol{q})$

$$\downarrow$$

$$\approx \left|F^{hi}_\lambda(\boldsymbol{q})\right|^2 \sum_{\boldsymbol{K},\boldsymbol{k},\boldsymbol{k'}}^{\lambda} F^{lo}_\lambda(\boldsymbol{k}) F^{lo}_\lambda(\boldsymbol{k'}) a^\dagger_{\frac{\boldsymbol{K}}{2}+\boldsymbol{k}} a^\dagger_{\frac{\boldsymbol{K}}{2}-\boldsymbol{k}} a_{\frac{\boldsymbol{K}}{2}-\boldsymbol{k'}} a_{\frac{\boldsymbol{K}}{2}+\boldsymbol{k'}}$$

Momentum distributions at low RG resolution

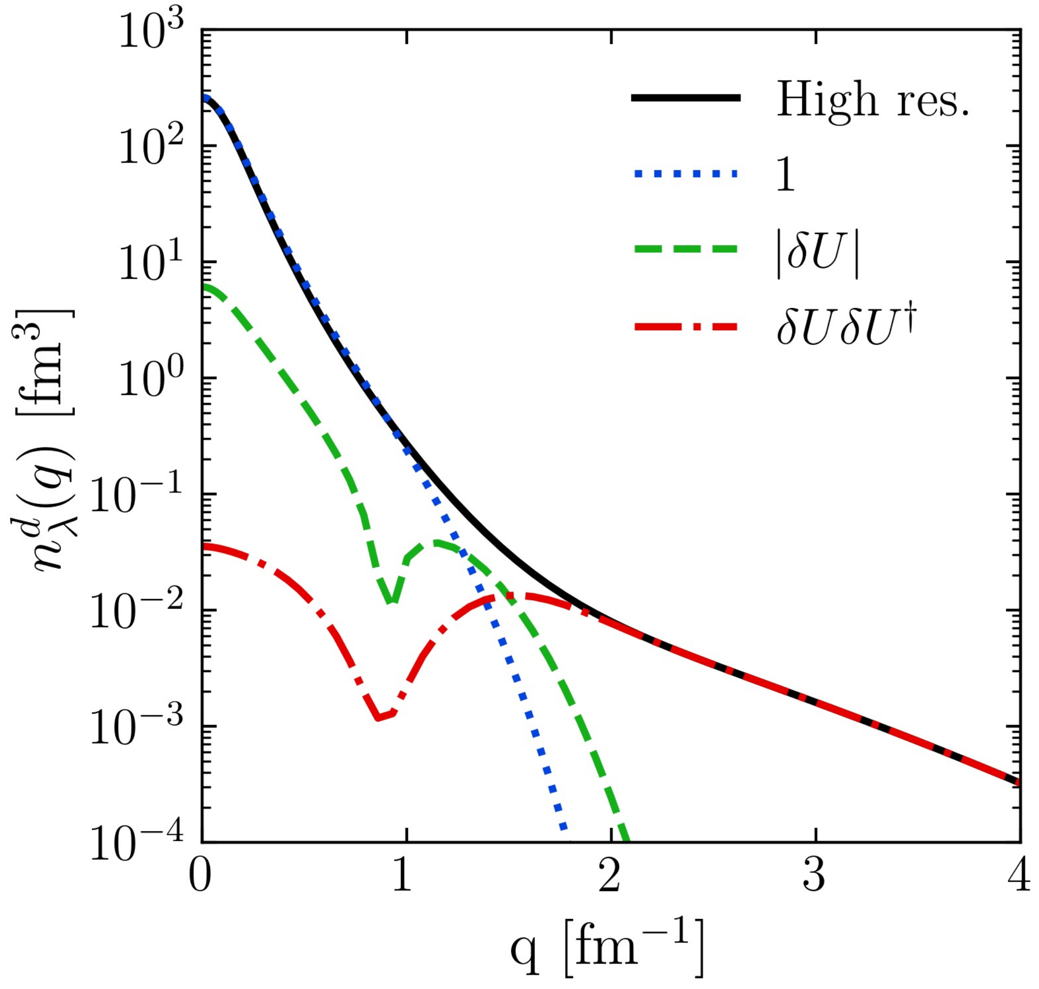

Fig. 2: Contributions to deuteron momentum distribution with AV18 and $\lambda = 1.35$ fm^{-1}.

- For high-q, the $\delta U_\lambda \delta U_\lambda^\dagger$ 2-body term dominates

$$\approx \sum \delta U_\lambda(\boldsymbol{k},\boldsymbol{q})\delta U_\lambda^\dagger(\boldsymbol{q},\boldsymbol{k}')a^\dagger_{\frac{\boldsymbol{K}}{2}+\boldsymbol{k}}a^\dagger_{\frac{\boldsymbol{K}}{2}-\boldsymbol{k}}a_{\frac{\boldsymbol{K}}{2}-\boldsymbol{k}'}a_{\frac{\boldsymbol{K}}{2}+\boldsymbol{k}'}$$

Apply this strategy to nuclear momentum distributions using local density approximation (LDA)!

$F_\lambda^{hi}(\boldsymbol{q})$

$$\approx \left|F_\lambda^{lo}(\boldsymbol{q})\right|^2 \sum_{\boldsymbol{K},\boldsymbol{k},\boldsymbol{k}'} F_\lambda^{lo}(\boldsymbol{k})F_\lambda^{lo}(\boldsymbol{k}')a^\dagger_{\frac{\boldsymbol{K}}{2}+\boldsymbol{k}}a^\dagger_{\frac{\boldsymbol{K}}{2}-\boldsymbol{k}}a_{\frac{\boldsymbol{K}}{2}-\boldsymbol{k}'}a_{\frac{\boldsymbol{K}}{2}+\boldsymbol{k}'}$$

[1]R.B. Wiringa et al., Phys. Rev. C **89**, 024305 (2014)
https://www.phy.anl.gov/theory/research/momenta/
[2]K. Bennaceur et al., Comput. Phys. Commun. **168**, 96 (2005)

Proton momentum distributions

- Low RG resolution calculations reproduce momentum distributions of AV18 data[1] (high RG resolution calculation)

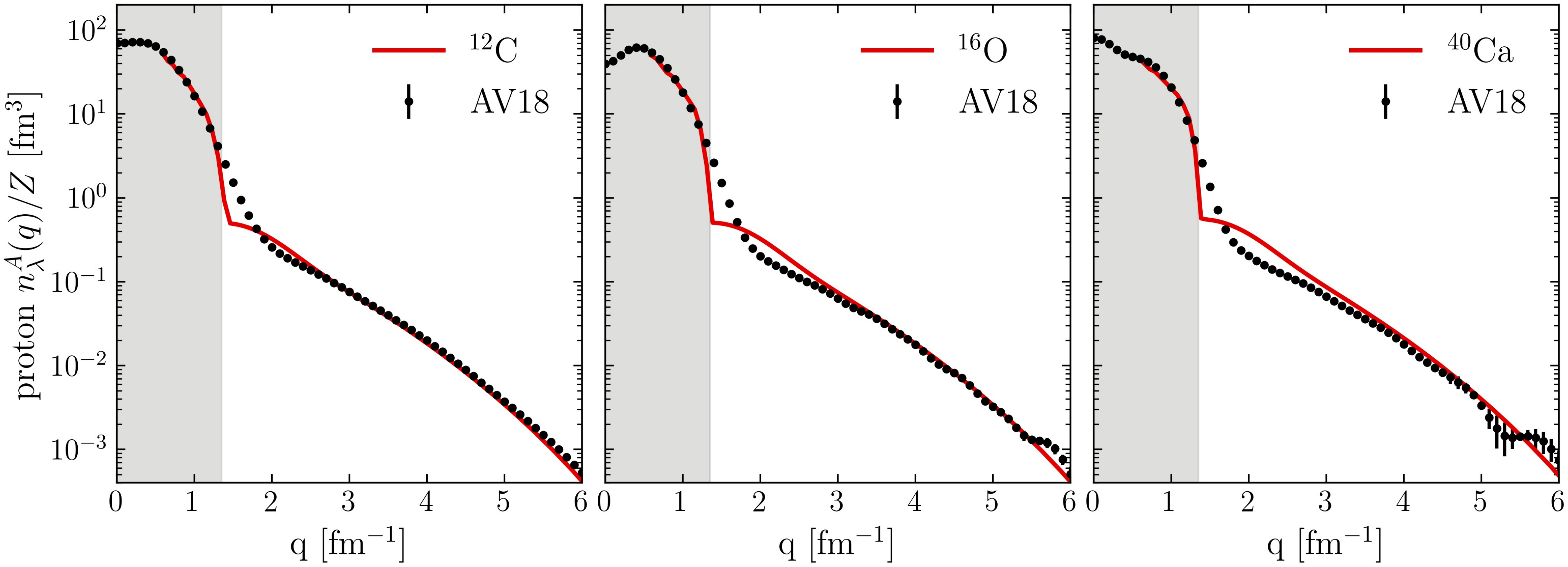

Fig. 3: Proton momentum distributions for ^{12}C, ^{16}O, and ^{40}Ca under LDA with AV18, $\lambda = 1.35$ fm^{-1}, and densities from Skyrme EDF SLy4 using the HFBRAD code[2].

[1]R.B. Wiringa et al., Phys. Rev. C **89**, 024305 (2014)
https://www.phy.anl.gov/theory/research/momenta/
[2]K. Bennaceur et al., Comput. Phys. Commun. **168**, 96 (2005)

Proton momentum distributions

- Universality: High-q dependence from universal function $\approx \left|F_\lambda^{hi}(q)\right|^2$ fixed by 2-body and insensitive to nucleus

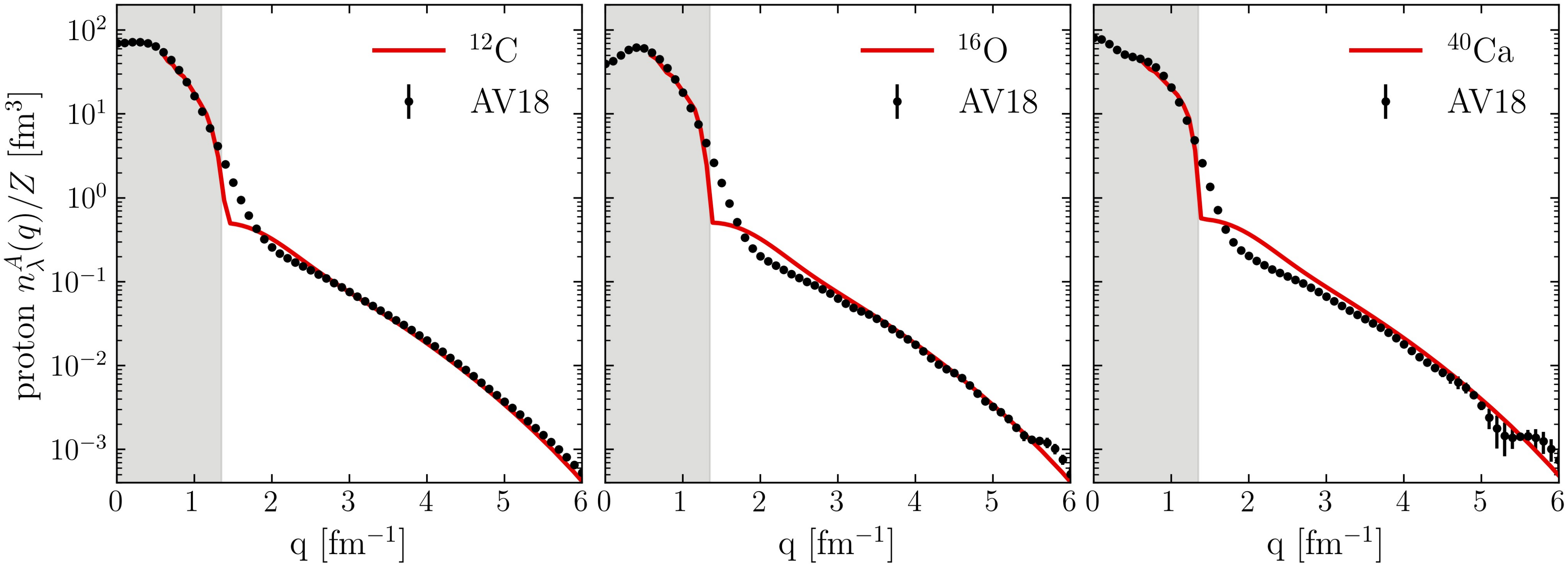

Fig. 3: Proton momentum distributions for ^{12}C, ^{16}O, and ^{40}Ca under LDA with AV18, $\lambda = 1.35$ fm^{-1}, and densities from Skyrme EDF SLy4 using the HFBRAD code[2].

[1]R.B. Wiringa et al., Phys. Rev. C **89**, 024305 (2014)
https://www.phy.anl.gov/theory/research/momenta/
[2]K. Bennaceur et al., Comput. Phys. Commun. **168**, 96 (2005)

Proton momentum distributions

- Universality: High-q dependence from universal function $\approx \left|F_\lambda^{hi}(q)\right|^2$ fixed by 2-body and insensitive to nucleus

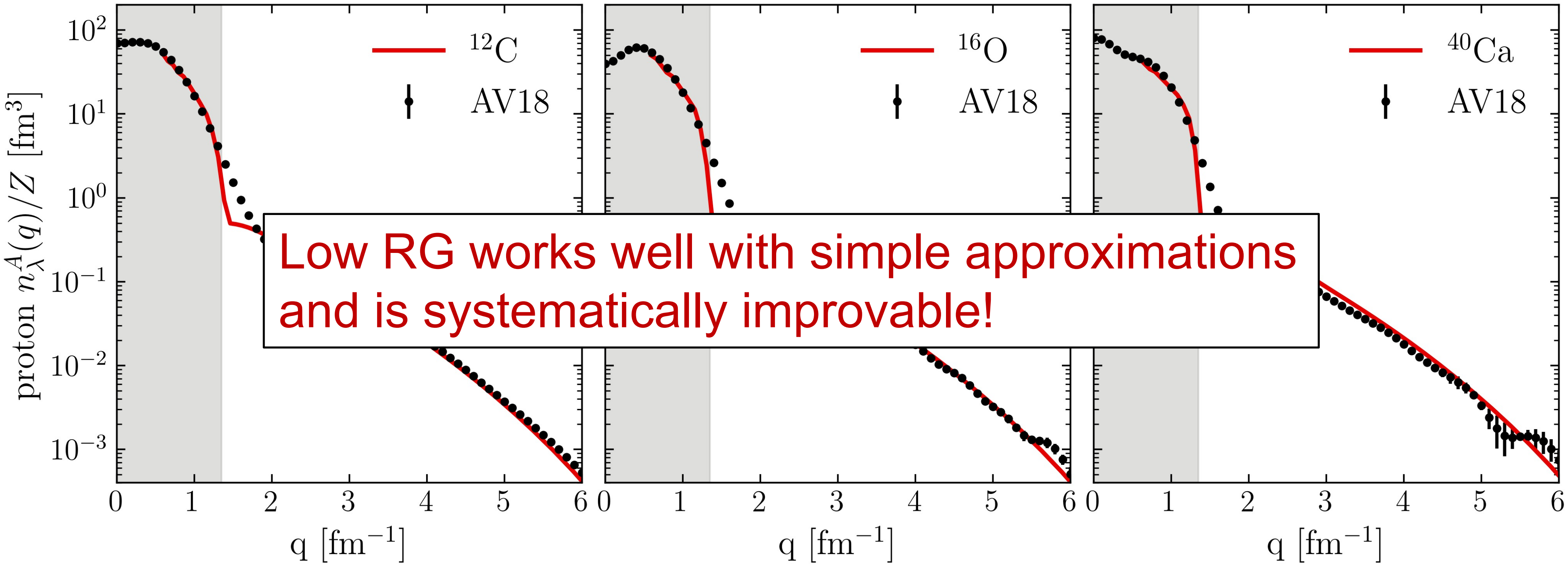

Fig. 3: Proton momentum distributions for ^{12}C, ^{16}O, and ^{40}Ca under LDA with AV18, λ = 1.35 fm^{-1}, and densities from Skyrme EDF SLy4 using the HFBRAD code[2].

SRC scaling factors

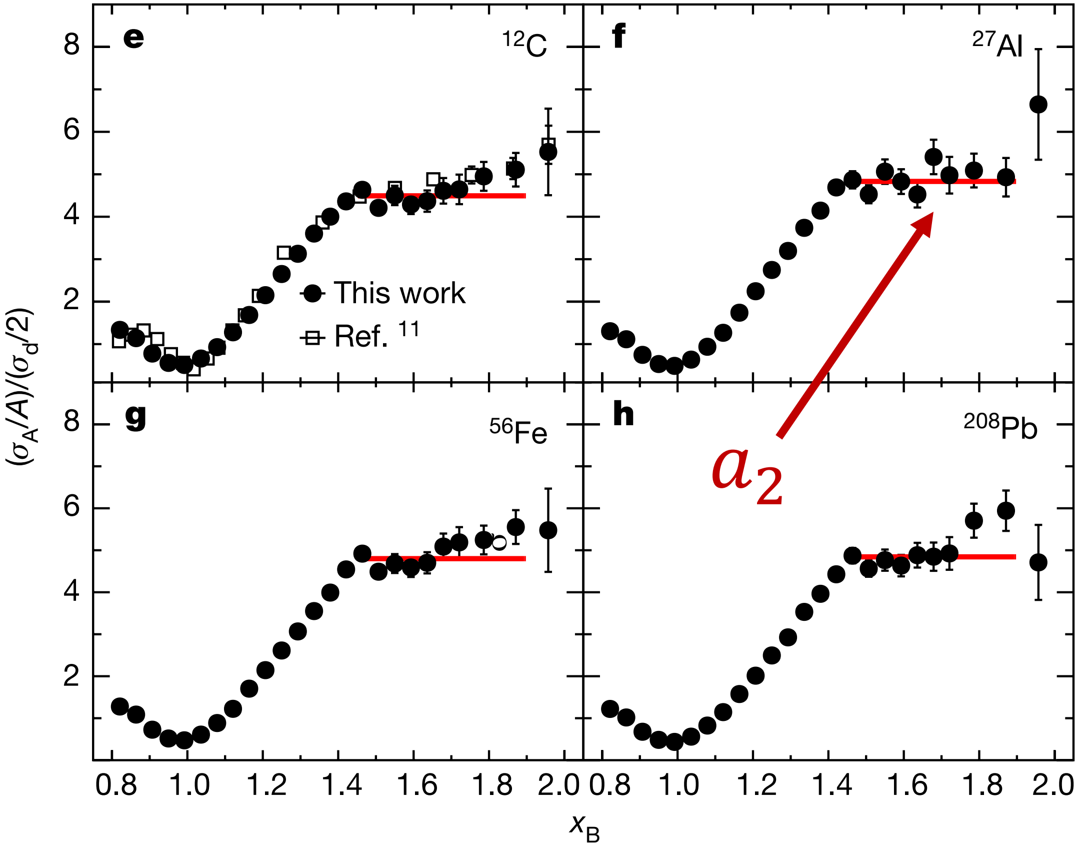

Fig. 4: Ratio of per-nucleon electron scattering cross section of nucleus A to that of deuterium, where the red line indicates a constant fit. Figure from B. Schmookler et al. (CLAS), Nature **566**, 354 (2019).

- SRC scaling factors a_2 defined by plateau in cross section ratio $\frac{2\sigma_A}{A\sigma_d}$ at $1.45 \leq x \leq 1.9$
- Extract a_2 from momentum distributions

$$a_2 = \lim_{q \to \infty} \frac{P^A(q)}{P^d(q)} \approx \frac{\int_{\Delta p^{high}} dq P^A(q)}{\int_{\Delta p^{high}} dq P^d(q)}$$

where $P^A(q)$ is the single-nucleon probability distribution in nucleus A

[1]E. Chabanat et al., Nucl. Phys. A **635**, 231 (1998)
[2]J. Decharge et al., Phys. Rev. C **21**, 1568 (1980)
[3]B. Schmookler et al. (CLAS), Nature **566**, 354 (2019)
[4]J. Ryckebusch et al., Phys. Rev. C **100**, 054620 (2019)

SRC scaling factors

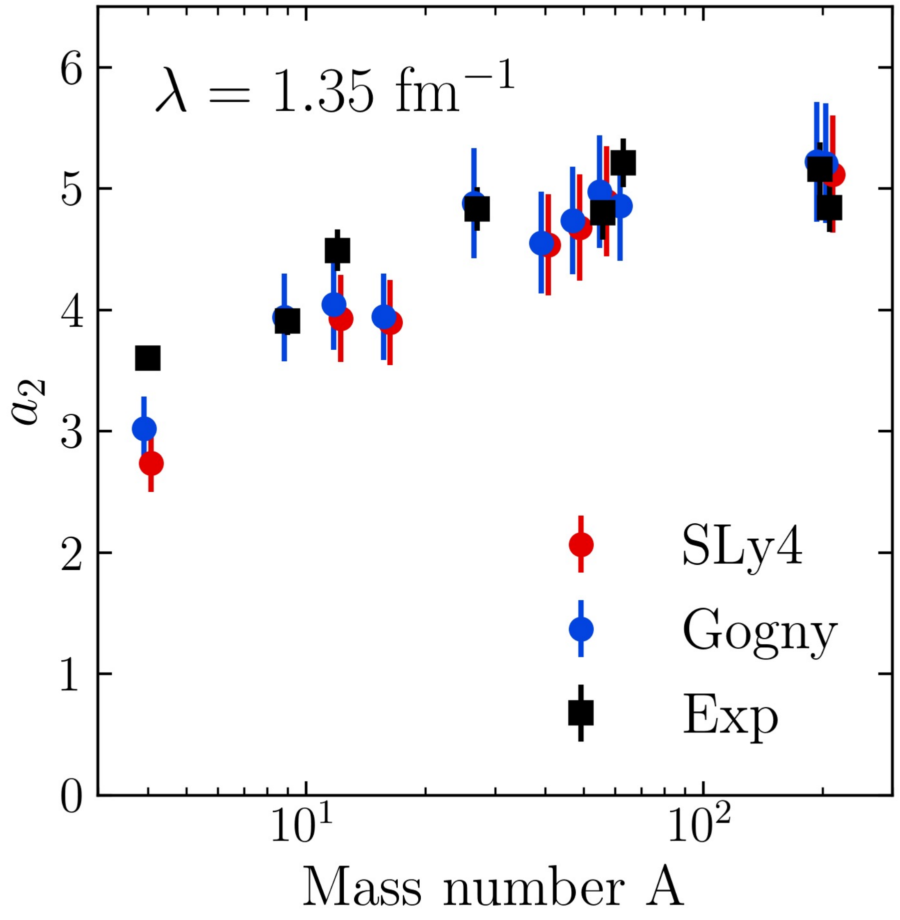

Fig. 5: a_2 scale factors using single-nucleon momentum distributions under LDA (SLy4 in red[1], Gogny[2] in blue) with AV18 and $\lambda = 1.35$ fm^{-1} compared to experimental values[3].

- SRC scaling factors a_2 defined by plateau in cross section ratio $\frac{2\sigma_A}{A\sigma_d}$ at $1.45 \leq x \leq 1.9$
- Extract a_2 from momentum distributions

$$a_2 = \lim_{q\to\infty} \frac{P^A(q)}{P^d(q)} \approx \frac{\int_{\Delta p^{high}} dq P^A(q)}{\int_{\Delta p^{high}} dq P^d(q)}$$

  where $P^A(q)$ is the single-nucleon probability distribution in nucleus A
- Good agreement with a_2 values from experiment[3] and LCA calculations[4]
- Error bars from varying Δp^{high}

SRC phenomenology

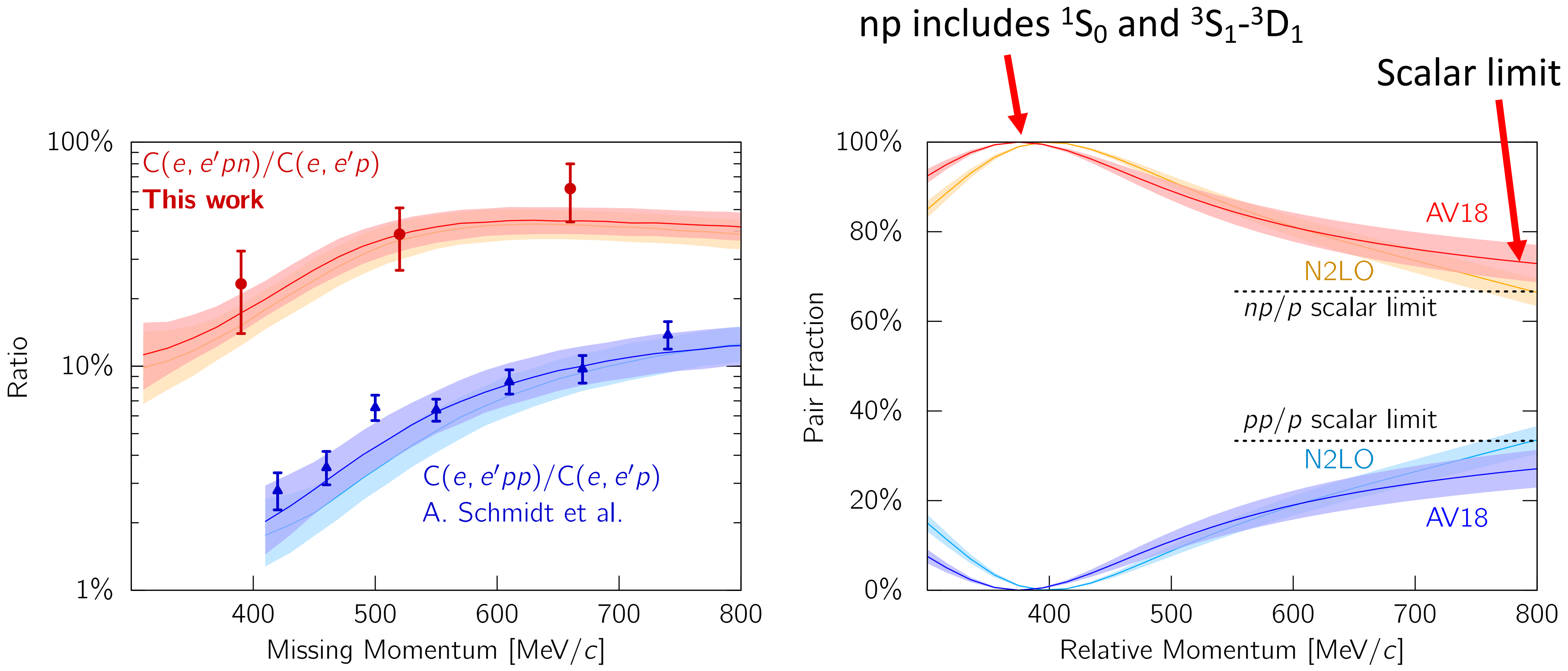

Fig. 6: (a) Ratio of two-nucleon to single-nucleon electron-scattering cross sections for carbon as a function of missing momentum. (b) Fraction of np to p and pp to p pairs versus the relative momentum. Figure from CLAS collaboration publication[1].

- At high RG resolution, the tensor force and the repulsive core of the NN interaction kicks nucleon pairs into SRCs
- np dominates because the tensor force requires spin triplet pairs (pp are spin singlets)
- Do we describe this physics at low RG resolution?

[1]I. Korover et al. (CLAS), arXiv:2004.07304 (2014)

SRC phenomenology

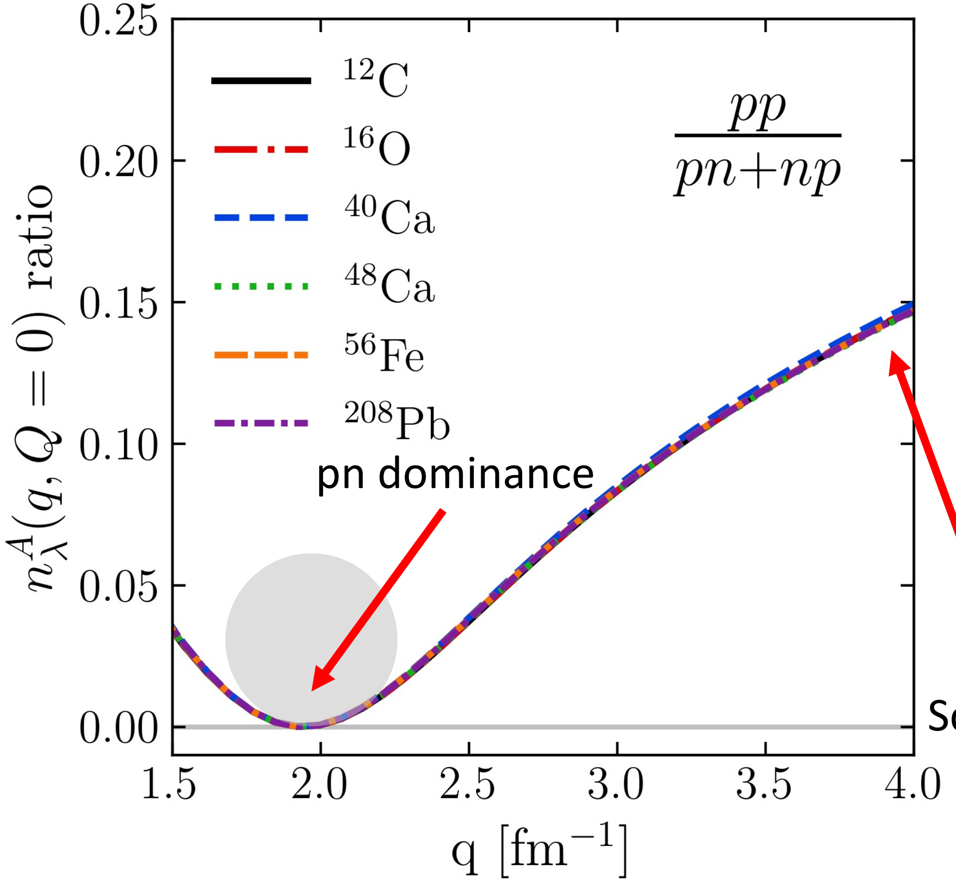

Fig. 7: pp/pn ratio of pair momentum distributions under LDA with AV18 and λ = 1.35 fm^{-1}.

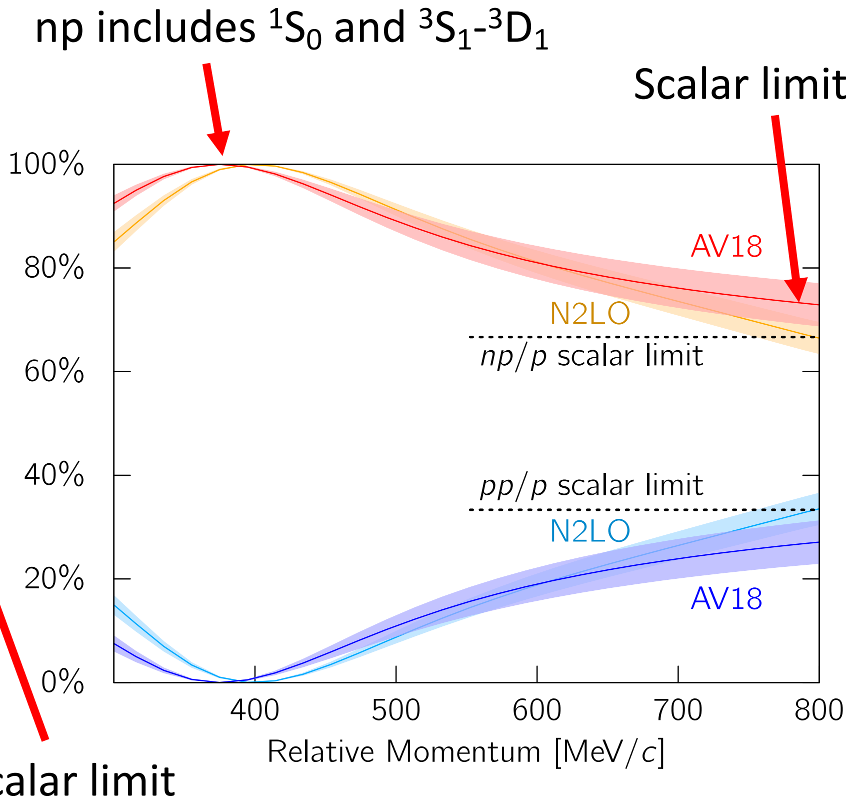

- At low RG resolution, SRCs are suppressed in the wave function and shifted into the operator
- Physics is established in the 2-body system – can apply to any nucleus!
- Low RG resolution picture reproduces the characteristics of cross section ratios using simple approximations

SRC phenomenology

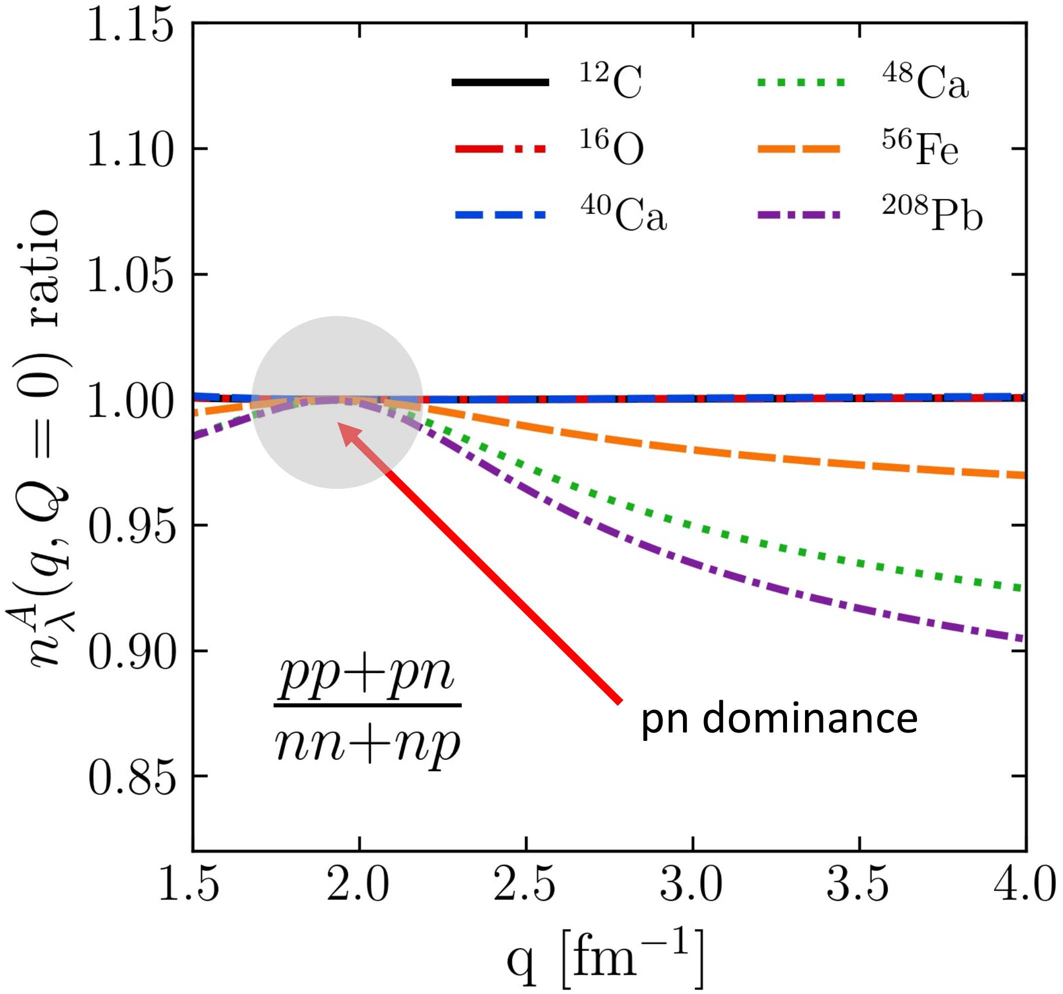

Fig. 8: (pp+pn)/(nn+np) ratio of pair momentum distributions under LDA with AV18 and $\lambda = 1.35$ fm^{-1}.

- Ratio ~1 independent of N/Z in pn dominant region
- Ratio < 1 for nuclei where N > Z and outside pn dominant region

Other exclusive knockout reactions

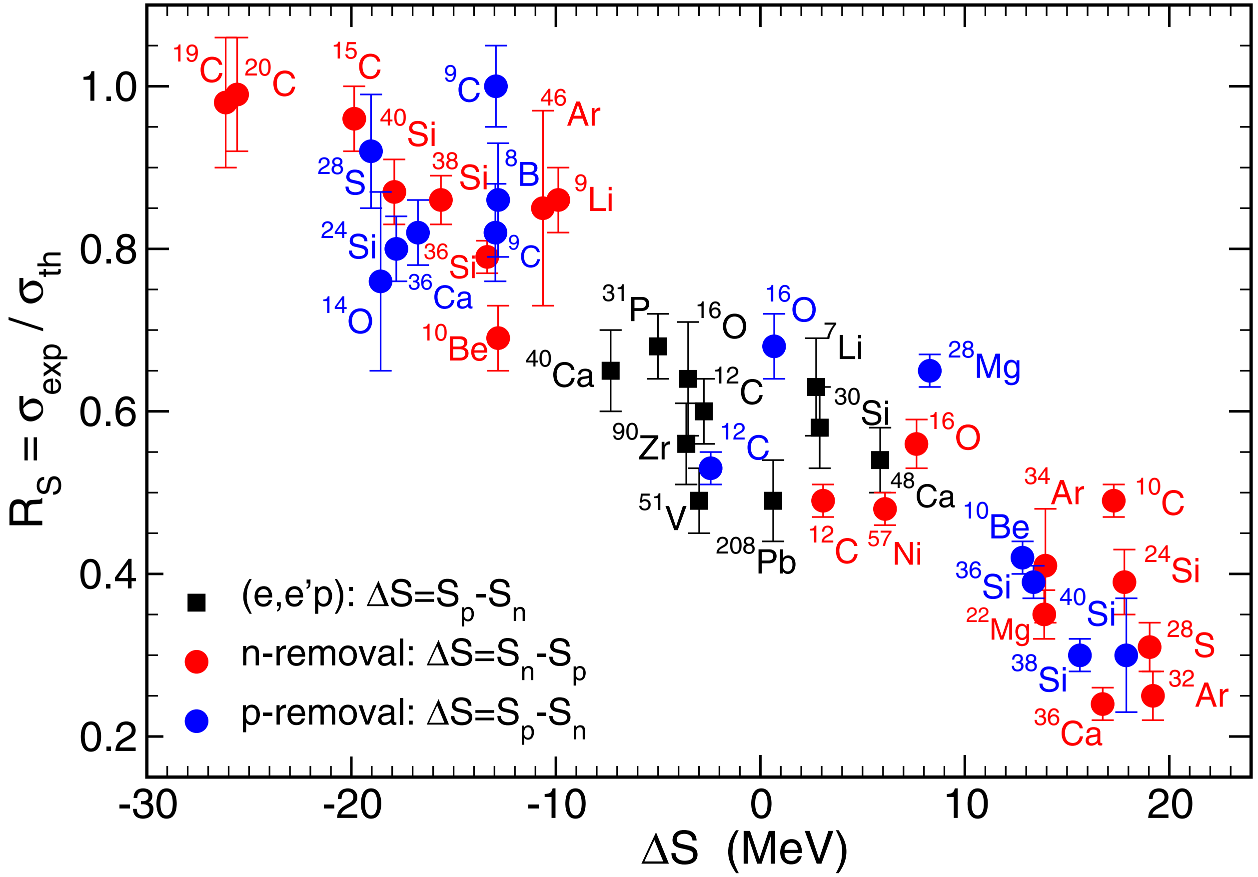

Fig. 9: R as a function of ΔS. Red (blue) points correspond to neutron-removal (proton-removal) cases. Solid black squares correspond to electron-induced proton knockout data. Figure from J. A. Tostevin and A. Gade, Phys. Rev. C **90**, 057602 (2014).

- RG analysis can help understand the cause of $R = \dfrac{\sigma_{exp}}{\sigma_{theory}} < 1$
- Mismatch of scale between one-body (high RG) operator and shell model structure (low RG) gives $\sigma_{theory} > \sigma_{exp}$

Other exclusive knockout reactions

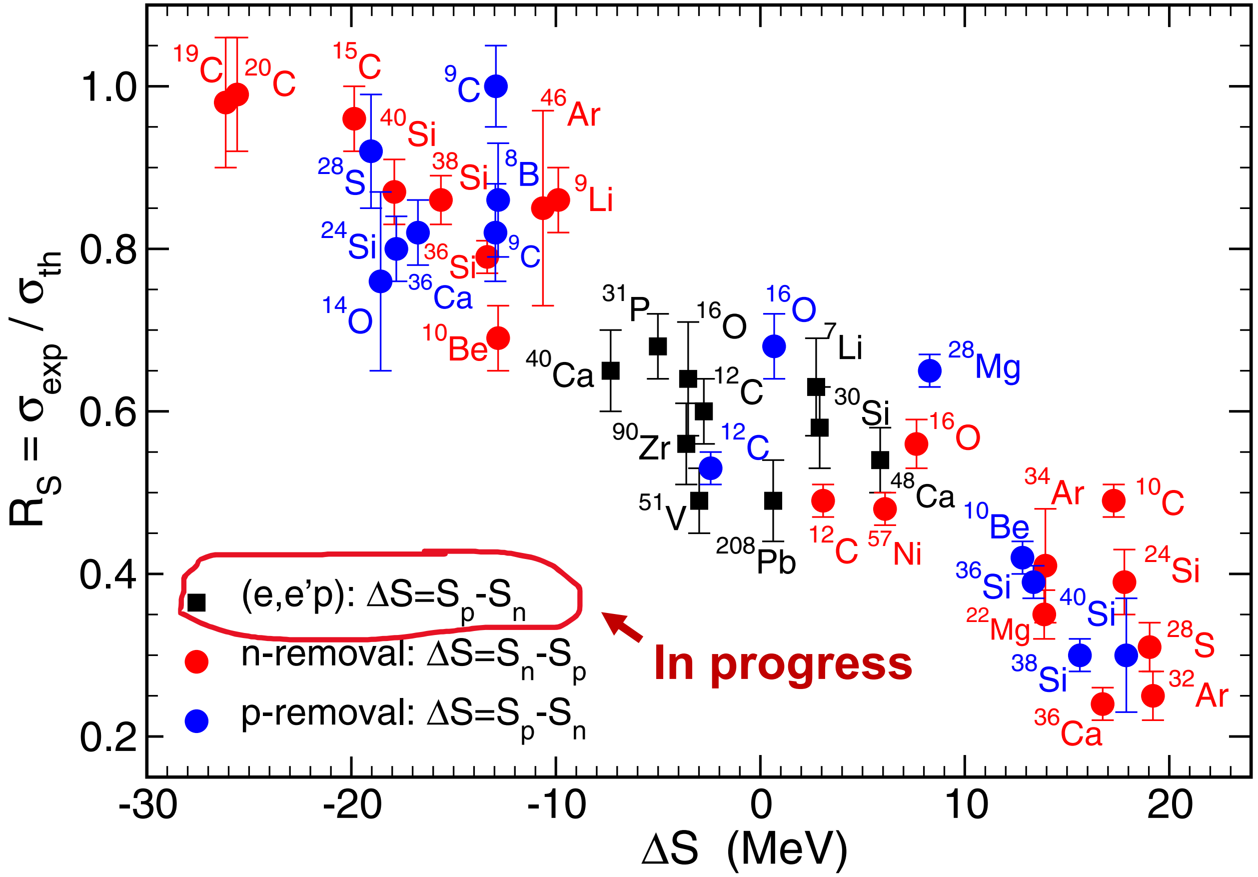

Fig. 9: R as a function of ΔS. Red (blue) points correspond to neutron-removal (proton-removal) cases. Solid black squares correspond to electron-induced proton knockout data. Figure from J. A. Tostevin and A. Gade, Phys. Rev. C **90**, 057602 (2014).

- RG analysis can help understand the cause of $R = \frac{\sigma_{exp}}{\sigma_{theory}} < 1$
- Mismatch of scale between one-body (high RG) operator and shell model structure (low RG) gives $\sigma_{theory} > \sigma_{exp}$
- Currently working on SRG-evolving spectroscopic factors for $(e, e'p)$ reactions
- Note, spectroscopic factors are scale/scheme dependent

Summary and outlook

- Simple approximations work and are systematically improvable at low RG resolution
- Results suggest that we can analyze high-energy nuclear reactions using low RG resolution structure (e.g., shell model) and consistently evolved operators
  - Matching resolution scale between structure and reactions is crucial!
- Ongoing work:
  - Extend to $(e, e'p)$ knockout cross sections and test scale/scheme dependence of extracted properties
  - Investigate impact of various corrections: 3-body terms, final state interactions, etc.
  - Apply to more complicated knock-out reactions (SRG with optical potentials)
  - Implement uncertainty quantification in low RG resolution calculations

Extras

Extras

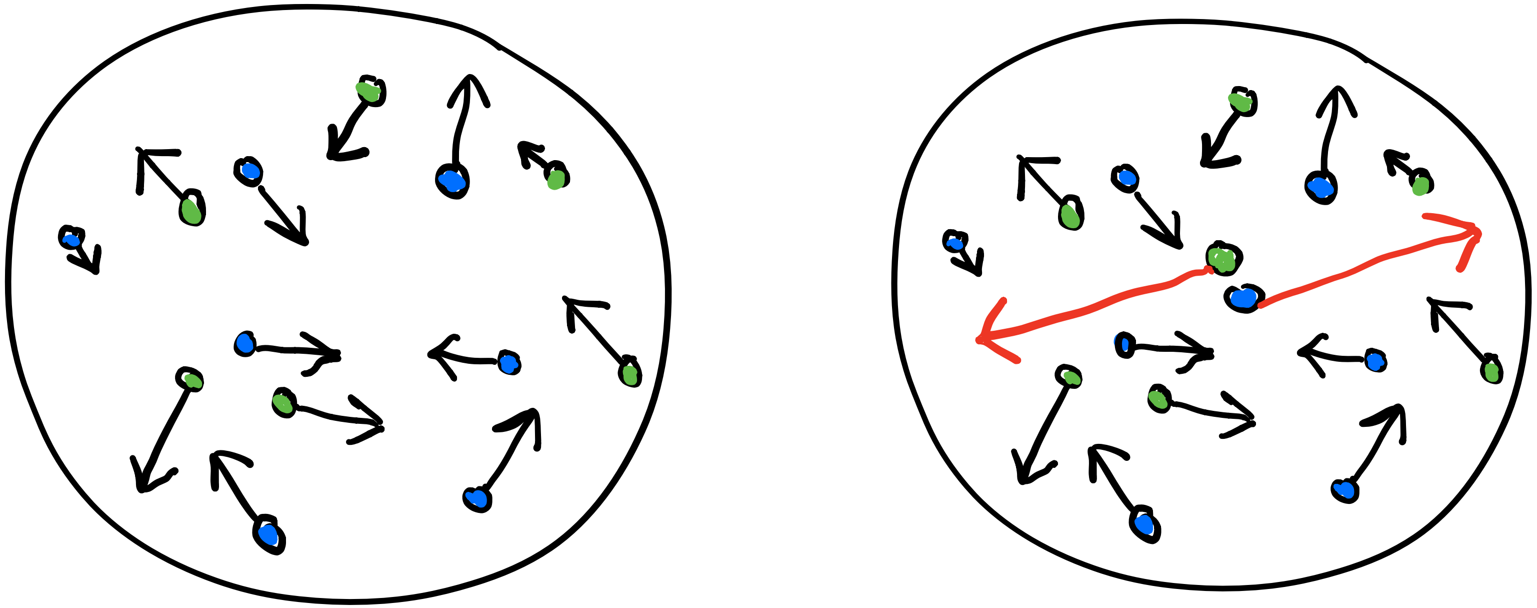

Fig. 10: Cartoon snapshots of a nucleus at (left) low-RG and (right) high-RG resolutions. The back-to-back nucleons at high-RG resolution are an SRC pair with small center-of-mass momentum.

SRG decoupling

- Evolve operators to low RG resolution

$$O(s) = U(s)O(0)U^{\dagger}(s)$$

where $s = 0 \to \infty$ and
$U(s)$ is unitary

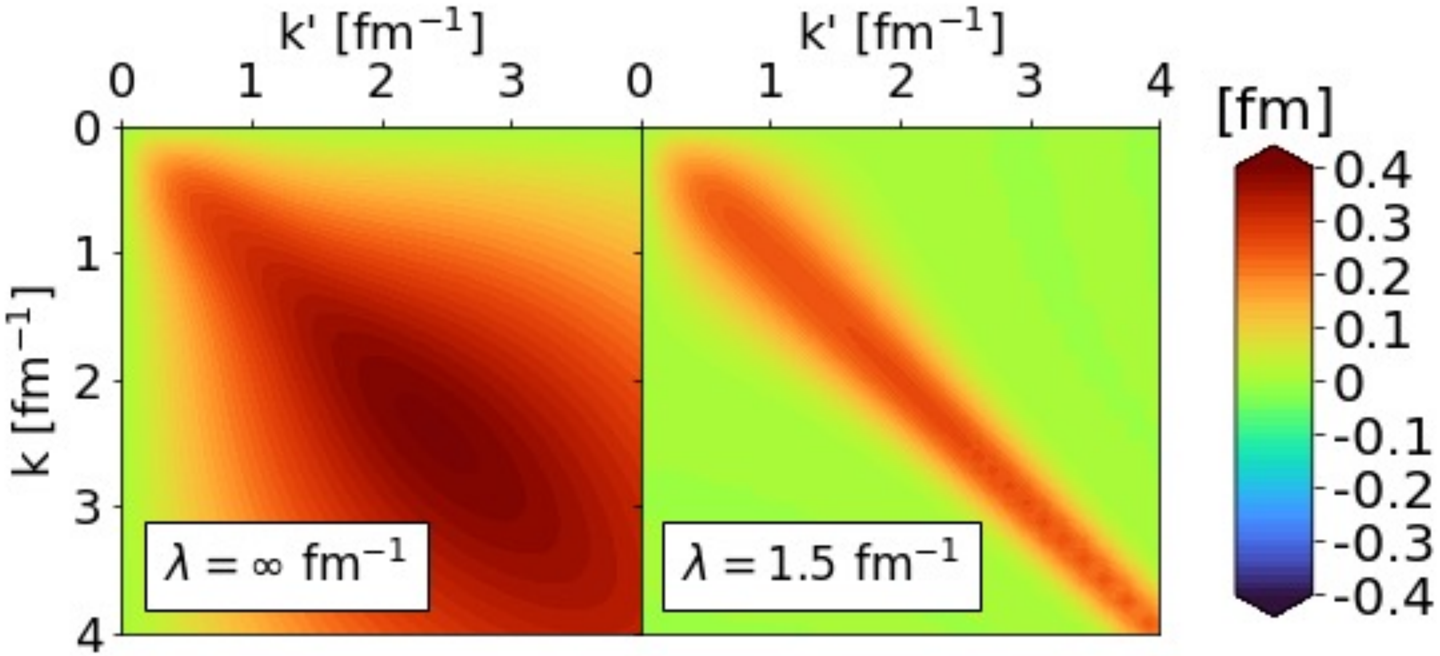

Fig. 11: Momentum space matrix elements of Argonne v18 (AV18) under SRG evolution in $^1P_1$ channel.

SRG decoupling

- Evolve operators to low RG resolution

$$O(s) = U(s)O(0)U^{\dagger}(s)$$

where $s = 0 \to \infty$ and $U(s)$ is unitary

- $\lambda = s^{-1/4}$ describes the decoupling scale of the RG evolved operator

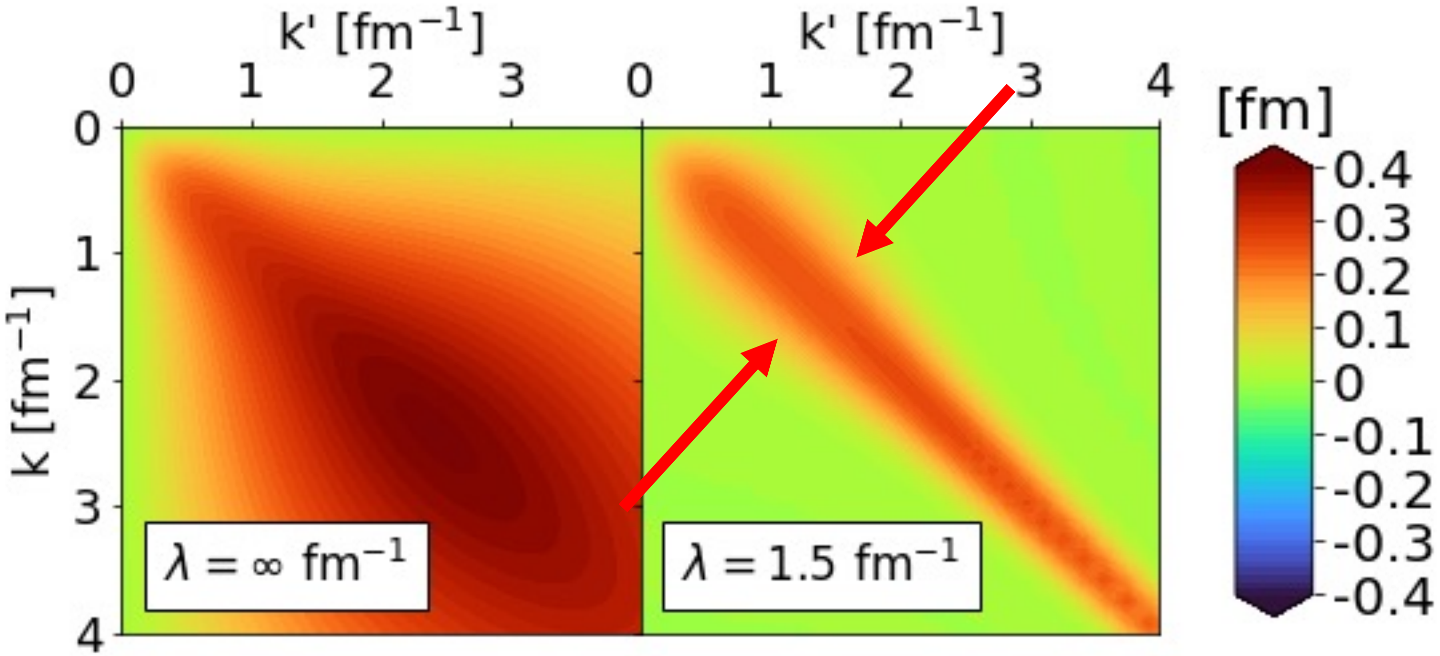

Fig. 11: Momentum space matrix elements of Argonne v18 (AV18) under SRG evolution in $^1P_1$ channel.

S-state and D-state contributions

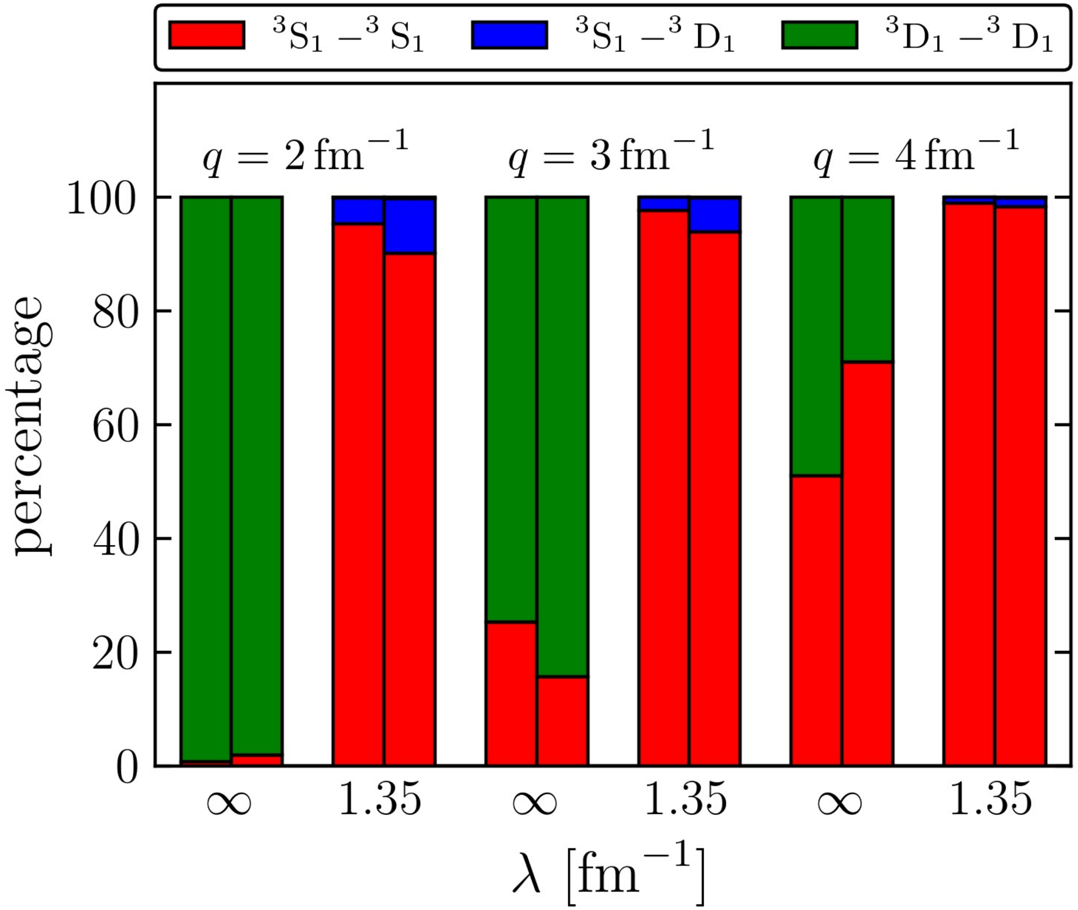

Fig. 12: Percentage contributions from each channel to the matrix element of the momentum distribution in the deuteron at several relative momentum values q for AV18 (left bar at each λ value) and Gezerlis N^{2}LO (right bar) potentials. We compare unevolved and SRG-evolved (both wave function and operator, so the net matrix element is unchanged) results where $\lambda = 1.35$ fm^{-1}

Factorization

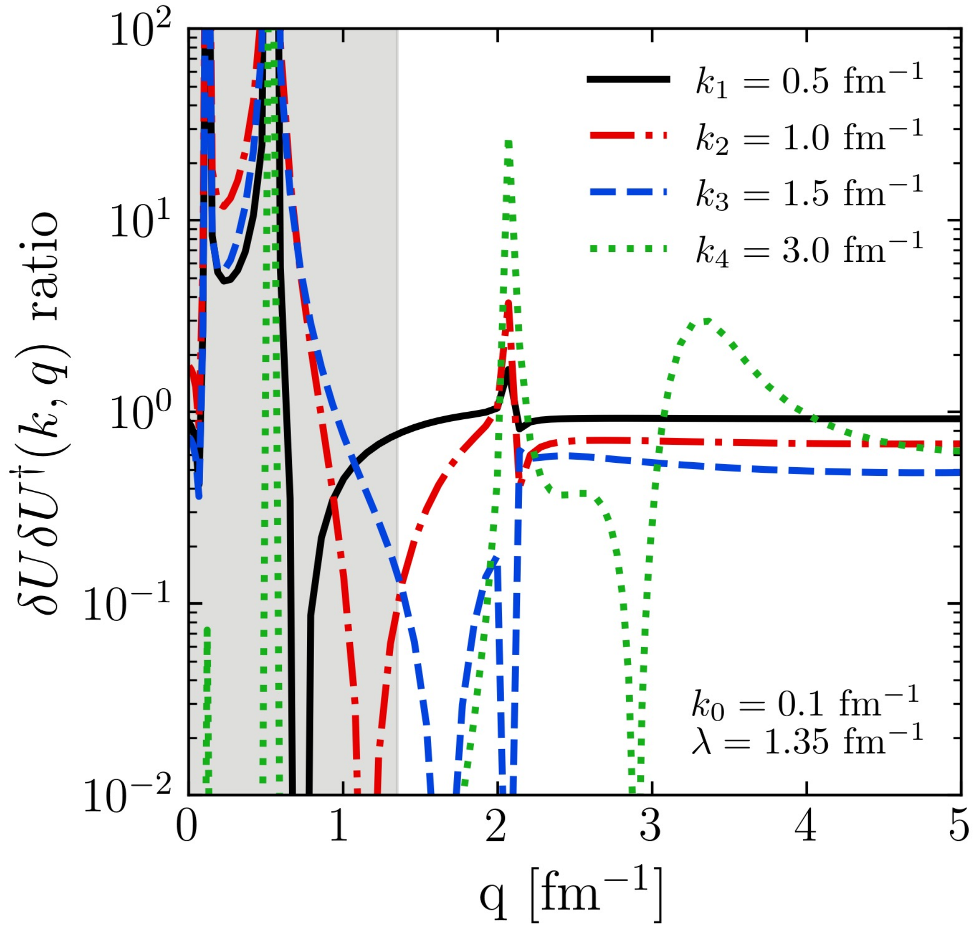

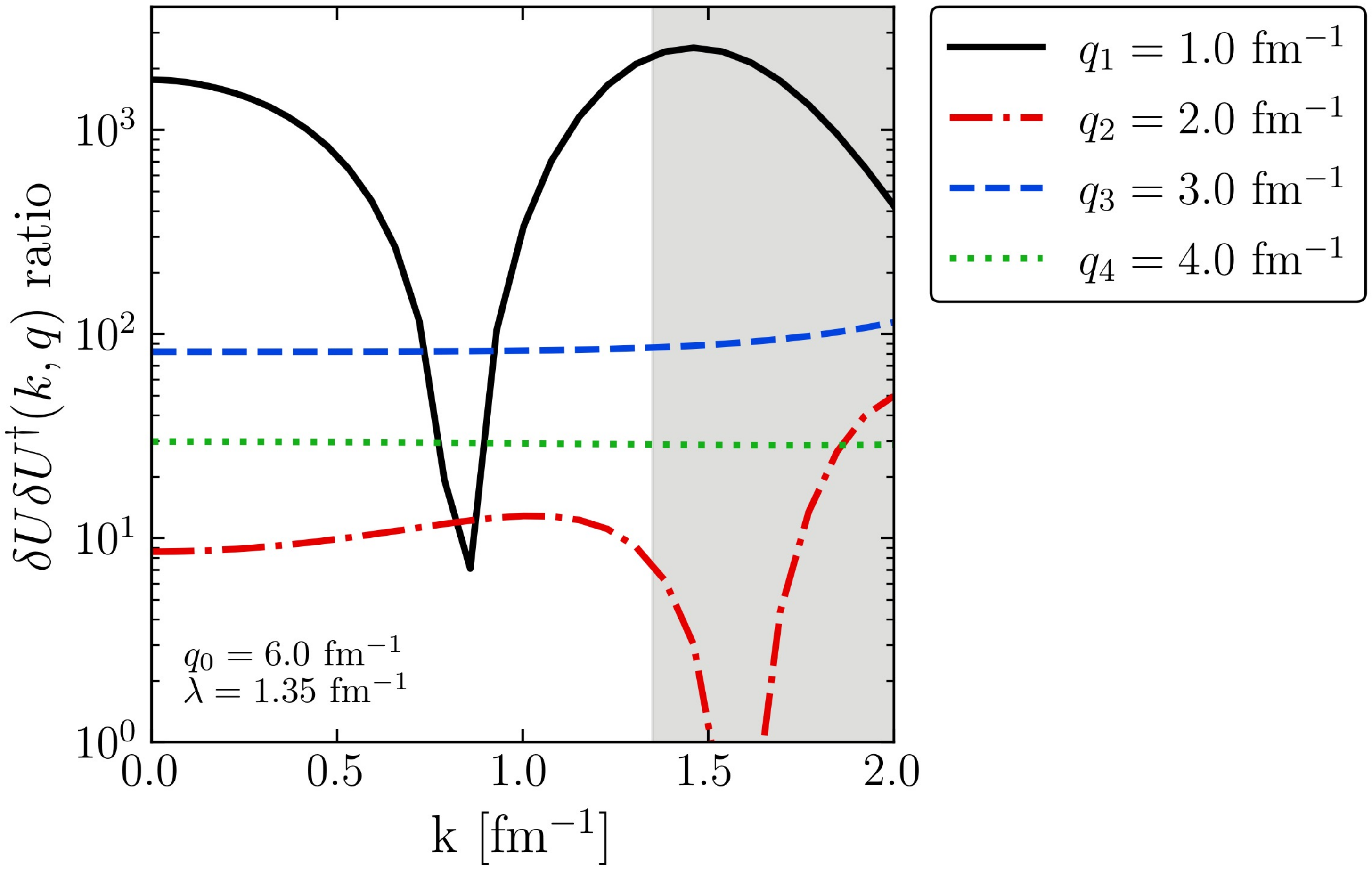

SRG λ dependence in momentum distributions